NANO LETTERS

LETTER

pubs.acs.org/NanoLett

Wulff Construction for Alloy Nanoparticles

E. Ringe,*,† R. P. Van Duyne,† and L. D. Marks‡

†Department of Chemistry and ‡Department of Materials Science and Engineering, Northwestern University, Evanston, Illinois 60201, United States

Supporting Information

ABSTRACT: The Wulff construction is an invaluable tool to understand and predict the shape of nanoparticles. We demonstrate here that this venerable model, which gives a size-independent thermodynamic shape, becomes size dependent in the nanoscale regime for an alloy and that the infinite reservoir approximation breaks down. The improvements in structure and energetic modeling have wide-ranging implications both in areas where energetics govern (e.g., nucleation and growth) and where the surface composition is important (e.g., heterogeneous catalysis).

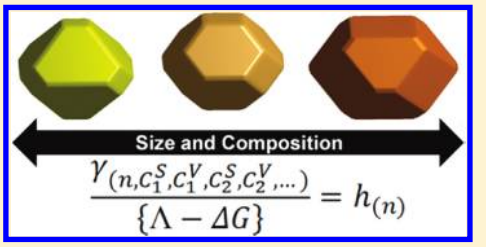

KEYWORDS: Alloy nanoparticles, thermodynamic modeling, Wulff construction, surface segregation, nanoparticle shape

One of the classic models to describe particle shape, whether small, large, free-standing, or as precipitates, is the Wulff construction,[1] which dictates a particle shape given its orientation-dependent surface free energy. On the basis of the original experimental observations of natural crystals by Wulff, the first mathematical explanations appeared during the second world war first by von Laue[2] with a more sophisticated proof given shortly after by Dinghas[3] and some applications to other cases by Herring.[4] Interest in the Wulff construction was recently renewed with the development of nanotechnology, as it can be applied to the understanding of many nanoparticle shapes.[5,6]

While there have been extensions such as the Winterbottom[7] construction, a modified form used for multiply twinned particles[8] and the SummerTop construction,[9] not too much has changed in the last decades for the Wulff construction, despite the accrued interest drawn by shape-controlled nanoparticle synthesis. One result for all such models is that the thermodynamic shape is size-independent, except in cases of exceptionally large strain effects[10,11] or counting effects related to edge and corner atoms.[12−14] In all cases deviations from the Wulff shape are relatively minor. While atomistic calculations are often used for small clusters, it is important to note that it has been clearly proved that the Wulff construction is a reliable tool for identifying the energetically most stable clusters in single-component systems beyond a few hundred atoms, from work where atomistic simulations have been carefully compared with continuum models.[14−18]

An interesting issue arises when one considers the same problem, the thermodynamic minimum energy shape of a particle, but now for an alloy in which there is the additional degree of freedom of surface segregation of one or more species. Nanoparticle alloys play a major role in catalysis.[19−21] A better understanding of the thermodynamics behind their shape and surface composition can be extremely beneficial in rational design of more efficient systems. Additionally, alloying provides a handle to tune plasmonic properties, as in the case of AgAu nanorods.[22] However, modeling of a nanoparticle alloy is still in its infancy, and pitfalls or limitations are often hard to avoid. In some cases it has been assumed a priori that the exposed surfaces always have full surface segregation to the lowest energy surface state[23,24] (the bulk acting effectively as an infinite reservoir) or the problem has been analyzed numerically using density functional theory, Monte Carlo simulations, and embedded atom methods for fixed shapes[25−30] with the surface composition allowed to vary, or for very small numbers of atoms. While such atomistic studies can provide invaluable information, there are of course approximations (sometimes severe) with the potentials, structures, and/or density functionals used. In addition, analytical techniques are often more powerful than atomistic ones as they provide solutions valid for different sizes, which is often hard to extract from an atomistic calculation.

In this paper we show that for an alloy an analytic solution exists for the thermodynamic equilibrium shape which is different from what one has for a single-component system. We first introduce and solve the "alloy Wulff construction", in which, strikingly, the shape and composition profile of the particle are dependent on size and the infinite reservoir approximation is invalid. Then we discuss its applicability and analyze appropriate examples.

To derive the alloy Wulff construction, we first define the contributions to the energy of the nanoparticle and then apply constraints to solve the resulting equations. A detailed derivation can be found in the Supporting Information.

The face- and composition-dependent surface free energy, $\gamma_{(n,C_1^S,C_1^V,C_2^S,C_2^V,\ldots)}$, is defined as the excess energy per unit area due to the presence of a surface. The total surface energy of the particle, E^S, is related by a truncated Taylor series expansion to

Received: May 28, 2011
Revised: July 6, 2011
Published: July 11, 2011

dx.doi.org/10.1021/nl2018146 | *Nano Lett.* 2011, 11, 3399–3403

$\gamma_{(n,C_1^S,C_1^V,C_2^S,C_2^V,\ldots)}$ and its derivative, the surface chemical potential, μ_i^S, as follows

$$E^S = \int (\gamma_{(n,C_1^S,C_1^V,C_2^S,C_2^V,\ldots)} + \sum \mu_i^S(x_i^S))\, dS \quad (1)$$

where n is the crystallographic face, C_i^S is the surface fractional concentration of element i, C_i^V is the bulk fractional concentration of element i, and x_i^S is a small change in surface composition. Note that the surface free energy must include a term correcting for the composition difference between bulk and surface, i.e.

$$\gamma_{(n,C_1^S,C_1^V,C_2^S,C_2^V,\ldots)} = \gamma_{(n,C_1^S,S_2^S,\ldots)} + \tau(G_{(C_1^S,C_2^S,\ldots)} - G_{(C_1^V,C_2^V,\ldots)}) \quad (2)$$

where τ is the surface thickness, $\gamma_{(n,C_1^S,C_2^S,\ldots)}$ is the free energy of a surface of concentration C_1^S, C_2^S, ... on a bulk of the same concentration, and $\gamma_{(n,C_1^S,C_1^V,C_2^S,C_2^V,\ldots)}$ is the free energy of a surface of concentration C_1^S, C_2^S, ... on a bulk of concentration C_1^V, C_2^V, ... The alloy bulk free energy, G, is defined as the deviation from a linear variation of bulk free energy per unit volume between two pure components.

Analogously, the change in bulk free energy, E^V, is expressed as

$$E^V = \int (\Delta G + \sum \mu_i^V(x_i^V))\, dV \quad (3)$$

where μ_i^V is the bulk chemical potential of component i and x_i^V is a small change in bulk composition. The bulk free energy term ΔG is the difference between the free energy per unit volume of the final bulk concentration C_1^V, C_2^V, ... and that of the initial composition, assuming equal surface and bulk concentration (which we will call homogeneous), B_1^V,B_2^V, ...

$$\Delta G = G_{(V_1^V,C_2^V,\ldots)} - G_{(B_1^V,B_2^V,\ldots)} \quad (4)$$

This term is crucial in the thermodynamic behavior of alloy nanoparticles, as surface segregation not only affects the surface but also starves the bulk of the segregating species. If the bulk is assumed to be an infinite reservoir, this term is zero, an approximation which as we will see is not always appropriate.

Conservation of mass, volume, and composition constraints are then applied, and the energy is minimized with respect to changes in bulk and surface concentration using a Lagrangian multiplier Λ as

$$F = \int \gamma_{(n,C_1^S,C_1^V,C_2^S,C_2^V,\ldots)}\, dS + \int (\Delta G - \Lambda)\, dV + \Lambda A \quad (5)$$

Solving eq 5 (see Supporting Information) yields the alloy Wulff construction

$$\frac{\gamma_{(n,C_1^S,C_1^V,C_2^S,C_2^V,\ldots)}}{\{\Lambda - \Delta G\}} = h(n) \quad (6)$$

which dictates the length of each face-dependent equilibrium surface normal $h_{(n)}$, i.e., the particle shape, as a function of surface composition, bulk composition, and particle size. The thermodynamic equilibrium energy is then simply the sum of the surface free energy and the change in bulk free energy

$$E_{tot} = E^S + E^V = \int \gamma_{(n,C_1^S,C_2^S,\ldots)}\, dS + \int \Delta G\, dV \quad (7)$$

Numerical analysis, performed in MATLAB (see Supporting Information) shows that two types of systems are possible, depending on the alloy strength. We can quantify alloy strength as the largest value of the difference between the linear interpolation of bulk free energy and the actual bulk free energy (G), divided by the linear interpolation value at that concentration. The first case is "weak" alloys, for which the maximum deviation is less than 1%, the largest value for AgAu being around 0.65%.[31−34] In such cases of small ΔG, the equilibrium shape approaches that of the traditional Wulff construction (supplementary eq 23, Supporting Information). Lowering of the surface free energy through surface segregation dominates for all concentrations: the segregating atoms go to the surface until the concentration where there are enough atoms to form a pure surface, and only after this does the bulk become an alloy. Note that very large surface free energy differences between possible surface compositions and a moderately weak alloying energy can also lead to this behavior. Analysis of AgPd (maximum deviation of 0.92%)[31,34−36] can be found in the Supporting Information because of its similarity to the weak alloy AgAu.

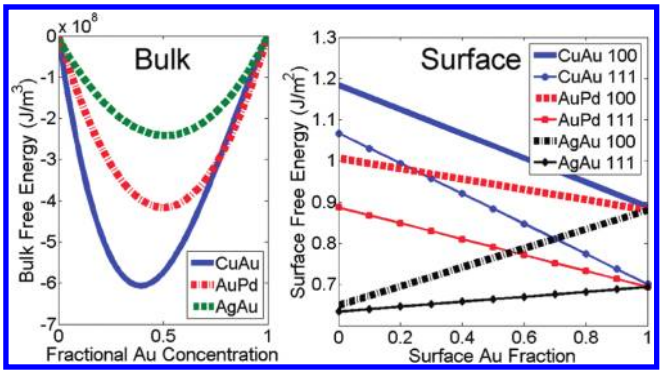

Figure 1. Bulk and surface free energy data for CuAu, AuPd, and AgAu. The bulk free energy is defined as the deviation from linearity between the two pure components, and the surface free energy is assumed to vary linearly between pure surfaces.

The second case is much more interesting and concerns "strong" alloys, for which the G term is above 1% at its maximum, and an infinite bulk reservoir approximation breaks down. Many bimetallic catalyst systems fall into this category: CuAu (maximum deviation of 1.2%)[19,31−33,37] and AuPd (maximum deviation of 1.1%),[31,32,36,38] for example, form disordered, segregating FCC alloys. Some of these alloys can form ordered phases at low temperatures, but we chose to ignore this effect as it is usually very weak at the relatively high temperatures considered.

Data used for the FCC random alloys CuAu[31−33,37] (720 K), AuPd[31,32,36,38] (600 K) and AgAu[31−34] (600 K) are presented in Figure 1 and Supplementary Table S1 (Supporting Information). The surface free energy and unit cell parameter were assumed to vary linearly between the two pure components. The surface thickness τ was assumed to be the distance between two equivalent planes, i.e., $c/2$ and $\sqrt{3}c/3$ for (100) and (111) faces, respectively. Identical segregation for all faces was assumed, but simple modifications can allow modeling of different segregation, as well as segregation gradients.

At all compositions, the surface free energies of the FCC alloys CuAu, AgAu, and AuPd dictate a thermodynamic shape dominated by (111) faces, with small (100) faces and no (110), yielding a structure between that of a cuboctahedron and an octahedron (Figure 2). With this geometry, the only parameter necessary to describe the particle shape is the ratio of surface normals h_{111}/h_{100}. Plotting this as a function of homogeneous

dx.doi.org/10.1021/nl2018146 |Nano Lett. 2011, 11, 3399–3403

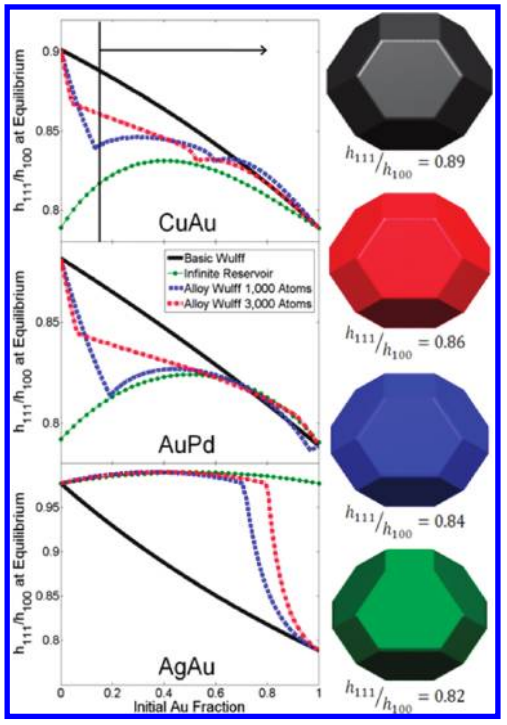

Figure 2. Shape dependence on composition and size according to the alloy Wulff model. (a) Size and composition dependence of the particle shape computed for a homogeneous alloy (basic Wulff), a segregating alloy with an infinite reservoir approximation, and the current alloy Wulff model. The shape is size-independent for homogeneous and infinite reservoir alloy nanoparticles. (b) Varying particle shape for CuAu alloys with initial Au fraction of 0.15.

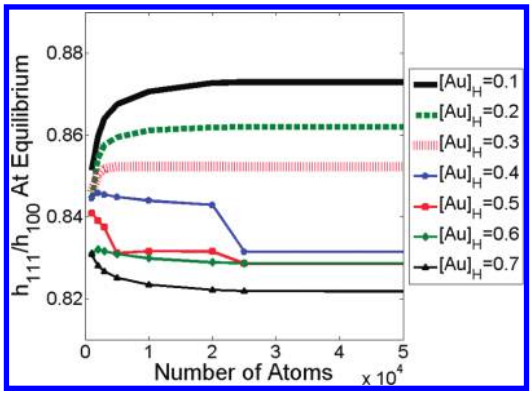

Figure 3. Size dependence of CuAu nanoparticle shape for different initial Au concentration ($[Au]_H$) according to the alloy Wulff model.

(initial) concentration for different particle sizes and compositions (Figures 2 and 3), a striking trend is apparent; the equilibrium morphology of a small alloy particle is size-dependent, unlike that of particles modeled either with the basic Wulff construction or with an alloy Wulff in which bulk free energy changes are neglected (infinite reservoir approximation).

The surface/bulk energy duality leads to the formation of up to three distinct composition−structure regimes with size-dependent boundaries, suggested in Figure 4. For CuAu, at small initial Au concentration (<10 atom %), the energy gained by lowering the surface free energy overwhelms any bulk free energy changes such that all the available Au segregates to the surface,

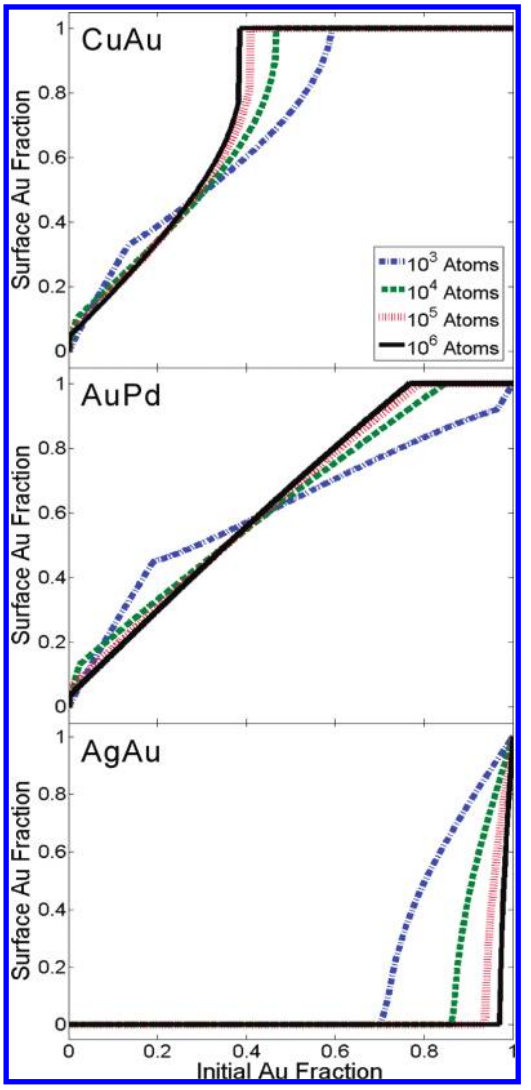

Figure 4. Effect of size and initial (homogeneous) composition on the equilibrium surface composition of alloy nanoparticles containing 10^3, 10^4, 10^5, and 10^6 atoms (~3, 7, 15, and 30 nm diameter). Three different regimes can be seen in CuAu and AuPd, while two regimes are observed for AgAu, as discussed in the text. The results for 10^6 atoms are very similar to those for larger (10^9 and 10^{12} atoms) particles; see Supporting Information for CuAu.

the bulk remains pure Cu, but there are never enough Au atoms to form a monolayer. This is a nanoscale effect, which is most important at small sizes, e.g., $<10^4$ atoms. As the initial Au concentration increases, the segregation (bulk) energy becomes comparable to the energy gained by surface compositional changes, and regime 2 starts. While a complete surface segregation may give the lowest surface free energy, it is prohibited by the large bulk free energy change it induces. The size-dependence of this transition, presented in Figure 4, becomes negligible for particles beyond 10^5 atoms (approximately 15 nm in diameter). The surface and bulk energy remain in balance until the concentration at which the latter can no longer prevent the formation of a pure surface. The second transition, from regime 2 to regime 3, results in a very sharp change in shape and concentration. This effect is also size dependent up to 10^6 atoms, as shown in Figures 3 and 4. Note that with an infinite reservoir approximation the surface composition is *always* that of regime 3, independent of size; the

dx.doi.org/10.1021/nl2018146 |*Nano Lett.* 2011, 11, 3399–3403

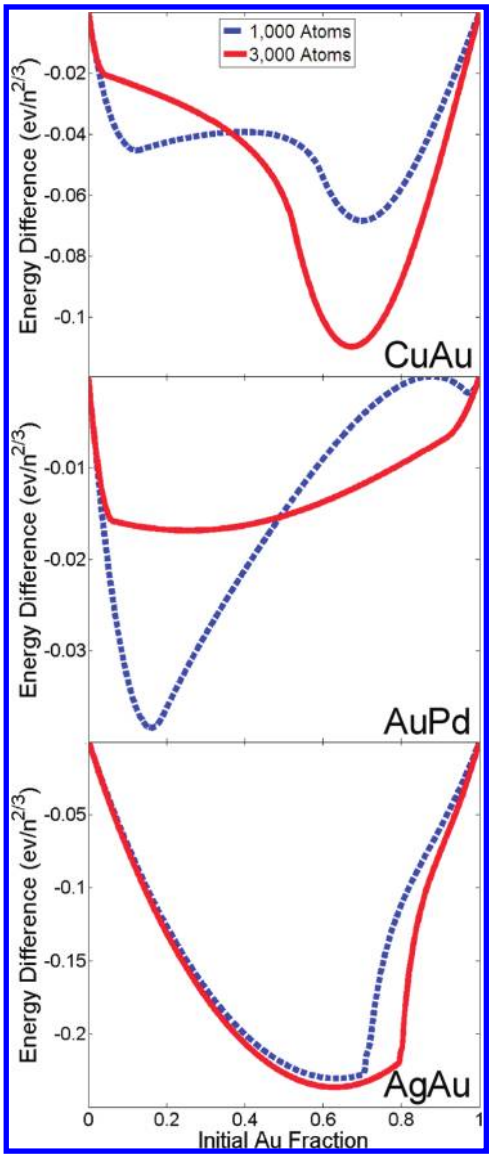

Figure 5. Energy difference between the traditional Wulff model and the alloy Wulff model, expressed in eV/(number of atoms$^{2/3}$). Notice that the Wulff model always yields the highest energy.

shape changes in this regime because the surface free energies depend upon the bulk concentration (eq 2). A similar behavior is observed for AuPd, except that at very small sizes, the bulk free energy changes effectively prevent the formation of a full monolayer of Au on the surface. AgAu, a weak alloy, behaves differently in that there is never a balance between surface and bulk energy, forming a pure Ag surface unless there are not enough atoms to do so. In other words, AgAu does not go through regime 2.

The behavior modeled by the alloy Wulff construction is significantly different than that of a homogeneous particle. Indeed, in the basic Wulff construction, lowering of energy through segregation is not allowed; thus the particle is practically never modeled at its equilibrium configuration. Figure 5 clearly shows that the total energy predicted by this simple model is always the highest. Because it includes energy-lowering shape (Figures 2 and 3) and composition changes (Figure 4) which the traditional Wulff and the infinite reservoir approximation neglect, the current model provides a better thermodynamic description of alloy nanoparticles.

We cannot unconditionally connect all possible cases of the alloy Wulff construction with experimental data since the effects we predict here have not (yet) been looked for (a future experimental challenge), but what evidence we can find is circumstantially strong. For "weak" alloys, our model correctly predicts surface segregation. Formation of an Ag outer layer was observed in AgAu particles of diameters 21 ± 7 and 52 ± 36 nm, albeit the oxidizing environment also drives Ag to the surface.[39] Calcination at 200−400 °C of 20 nm AuPd particles of unspecified initial composition[40] led to the formation of a Pd surface due to the higher affinity of Pd for O at such temperatures. Subsequent reduction at 500 °C[40] yielded the composition we predict, namely a Au-enriched surface. Nearly pure Ag surfaces (95−100%) have been observed in bulk $Ag_{33}Pd_{67}$ by STM,[41] while Auger electron spectroscopy of bulk $Ag_{77}Pd_{23}$ gave mixed results, either with much Ag segregation or almost none, depending on the degree of data processing involved.[42] Morphology and composition profiles in "strong" alloy nanoparticles, which are uniquely modeled in the alloy Wulff construction, have been barely studied. Extended X-ray absorption fine structure was used to probe the environment around Cu and Au atoms in small (<10 nm) particles of the strong alloy CuAu with an homogeneous Au fraction of 0.56.[43] The results showed a lower average nearest neighbor for Au (11 vs 12), consistent with partial surface Au segregation, as predicted here (Figure 4). This indicates that bulk forces can indeed prevent full surface segregation, a component the alloy Wulff construction uniquely takes into account. Unfortunately, the specific particle size, hence the exact degree of segregation, was not determined, leaving open questions. While the information available clearly supports our model, it also points to the lack of systematic experimental studies of alloy nanoparticle composition; we note that this type of information should be accessible with aberration-corrected electron microscopes.

The new approach provided by the alloy Wulff model has a multitude of implications, many rather transformative. The large surface to volume ratio (~30% of atoms are on the surface for a 1,000 atom particle) of nanoparticles make them especially interesting for heterogeneous catalysis, in which small (2−10 nm) alloy particles are commonly used.[19−21] We expect the alloy Wulff model to be extremely useful for such particles: given the proper surface free energies under reaction conditions (including presence of surfactant, underpotential deposition, etc.), one can predict the ratio of crystallographic faces and the surface composition, both critical factors for activity. Another area of scientific interest that will benefit from this new model is that of alloy nanoparticle growth. Seed-mediated syntheses are popular because they tend to provide better shape control, and now it is possible to understand the composition and morphology of those seeds and study how this relates to the final product.

■ ASSOCIATED CONTENT

Supporting Information. Detailed derivation of Wulff construction for alloy nanoparticles, details on free energy and unit cell parameter values used, MATLAB code overview, results for AgPd and additional figures for CuAu. This material is available free of charge via the Internet at http://pubs.acs.org.

■ AUTHOR INFORMATION

Corresponding Author

*E-mail: emilieringe@u.northwestern.edu.

■ ACKNOWLEDGMENT

This work was supported by the NSF (CHE-0911145) and the NSF MRSEC (DMR-0520513) at the Materials Research Center of Northwestern University.

■ REFERENCES

(1) Wulff, G. *Z. Kristallogr. Mineral.* **1901**, *34*, 449–530.
(2) von Laue, M. *Z. Kristallogr.* **1943**, *105*, 124–133.
(3) Dinghas, A. *Z. Kristallogr.* **1944**, *105*, 304–314.
(4) Herring, C. *Phys. Rev.* **1951**, *82*, 87–93.
(5) Marks, L. D. *Rep. Prog. Phys.* **1994**, *57*, 603–649.
(6) Xia, Y.; Xiong, Y.; Lim, B.; Skrabalak, S. E. *Angew. Chem., Int. Ed.* **2009**, *48*, 60–103.
(7) Winterbottom, W. L. *Acta Metall.* **1967**, *15*, 303–310.
(8) Marks, L. D. *J. Cryst. Growth* **1983**, *61*, 556–566.
(9) Zia, R. K. P.; Avron, J. E.; Taylor, J. E. *J. Stat. Phys.* **1988**, *50*, 727–736.
(10) Hamilton, J. C.; Léonard, F.; Johnson, E.; Dahmen, U. *Phys. Rev. Lett.* **2007**, *98*, 236102.
(11) Cahn, J. W.; Carter, W. C. *Metall. Trans. A* **1996**, *27*, 1431–1440.
(12) Marks, L. D. *Surf. Sci.* **1985**, *150*, 358–366.
(13) Wang, S.-W.; Falicov, L. M.; Searcy, A. W. *Surf. Sci.* **1984**, *143*, 609–625.
(14) Hamilton, J. C. *Phys. Rev. B* **2006**, *73*, 125447.
(15) Cleveland, C. L.; Landman, U. *J. Chem. Phys.* **1991**, *94*, 7376–7396.
(16) Baletto, F.; Ferrando, R. *Rev. Mod. Phys.* **2005**, *77*, 371–423.
(17) Baletto, F.; Ferrando, R.; Fortunelli, A.; Montalenti, F.; Mollet, C. *J. Chem. Phys.* **2002**, *116*, 3856–3863.
(18) Valkealahti, S.; Manninen, M. *Phys. Rev. B* **1998**, *57*, 15533–15540.
(19) Bracey, C. L.; Ellis, P. R.; Hutchings, G. J. *Chem. Soc. Rev.* **2009**, *38*, 2231–2243.
(20) Raimondi, F.; Scherer, G. G.; Kötz, R.; Wokaun, A. *Angew. Chem., Int. Ed.* **2005**, *44*, 2190–2209.
(21) Guczi, L. *Catal. Today* **2005**, *101*, 53–64.
(22) Lee, K.-S.; El-Sayed, M. A. *J. Phys. Chem. B* **2006**, *110*, 19220–19225.
(23) Piccinin, S.; Zafeiratos, S.; Stampfl, C.; Hansen, T. W.; Hävecker, M.; Teschner, D.; Bukhtiyarov, V. I.; Girgsdies, F.; Knop-Gericke, A.; Schlögl, R.; Scheffler, M. *Phys. Rev. Lett.* **2010**, *104*, 035503.
(24) Hong, S.; Yoo, M. H. *J. Appl. Phys.* **2005**, *97*, 084315.
(25) Wang, G.; Van Hove, M. A.; Ross, P. N.; Baskes, M. I. *J. Chem. Phys.* **2004**, *121*, 5410–5422.
(26) Xiao, S.; Hu, W.; Luo, W.; Wu, Y.; Li, X.; Deng, H. *Eur. Phys. J. B* **2006**, *54*, 479–484.
(27) Wang, G.; Van Hove, M. A.; Ross, P. N.; Baskes, M. I. *Prog. Surf. Sci.* **2005**, *79*, 28–45.
(28) Wang, L.-L.; Johnson, D. D. *J. Am. Chem. Soc.* **2009**, *131*, 14023–14029.
(29) Dannenberg, A.; Gruner, M. K.; Hucht, A.; Entel, P. *Phys. Rev. B* **2009**, *80*, 245438.
(30) Shan, B.; Wang, L.; Yang, S.; Hyun, J.; Kapur, N.; Zhao, Y.; Nicholas, J. B.; Cho, K. *Phys. Rev. B* **2009**, *80*, 035404.
(31) Wang, H. Y.; Najafabadi, R.; Srolovitz, D. J.; Lesar, R. *Interface Sci.* **1993**, *1*, 7–30.
(32) Vitos, L.; Ruban, A. V.; Skriver, H. L.; Kollár, J. *Surf. Sci.* **1998**, *411*, 186–202.
(33) Kart, H. H.; Tomak, M.; Çağin, T. *Modell. Simul. Mater. Sci. Eng.* **2005**, *13*, 657–669.
(34) Spreadborough, J.; Christian, J. W. *J. Sci. Instrum.* **1959**, *36*, 116–118.
(35) Pratt, J. N. *Trans. Faraday Soc.* **1960**, *56*, 975–987.
(36) Rao, C. N.; Rao, K. K. *Can. J. Phys.* **1964**, *42*, 1336–1342.
(37) Orr, R. L. *Acta Metall.* **1960**, *8*, 489–493.
(38) Methfessel, M.; Hennig, D.; Scheffler, M. *Phys. Rev. B* **1992**, *46*, 4816–4829.
(39) Wang, A.-Q.; Liu, J.-H.; Lin, S. D.; Lin, T.-S.; Mou, C.-Y. *J. Catal.* **2005**, *233*, 186–197.
(40) Herzing, A. A.; Watanabe, M.; Edwards, J. K.; Conte, M.; Tang, Z.-R.; Hutchings, G. J.; Kiely, C. J. *Faraday Discuss.* **2008**, *138*, 337–351.
(41) Wouda, P. T.; Schmid, M.; Nieuwenhuys, B. E.; Varga, P. *Surf. Sci.* **1998**, *417*, 292–300.
(42) Reniers, F. *Surf. Interface Anal.* **1995**, *23*, 374–380.
(43) Meitzner, G.; Via, G. H.; Lytle, F. W.; Sinfelt, J. H. *J. Chem. Phys.* **1985**, *83*, 4793–4799.